Original Research Article

Application of Deep Learning Techniques in the Development of Predictive Maintenance and Fault Detection in Electric Motors

ABSTRACT

Over the last two decades, computer processing capacity and digital camera use have increased. As a result, the thermographic technique and thermal analysis have gained greater use in electromechanical maintenance due to the cheapness of measuring devices. At the same time, several new methods and applications of methodologies based on Deep Learning emerged, mainly with the use of images and videos. In this sense, this contribution aims to verify the applicability of using the deep learning technique of convolutional neural networks to classify patterns of thermographic images of a bench grinder. The methodology used was the realization of thermographic pictures of a bench grinder after starting up, without applying effort to its discs and after applying a load to its axis, causing an increase in temperature in its electrical motor. This procedure was used to induce a temperature increase in the grinding machine housing since some types of faults in electric motors can be diagnosed due to ~~overtemperature~~over temperature by thermographic inspection. Furthermore, aPython-based computational codewas developed using a convolutional neural network that could differentiate the grinder's work profiles from the images with their respective thermal profiles. In conclusion, the technique proved promising for diagnosing motor failures by thermographyand can be implemented in automatic predictive maintenance routines.

Keywords: Thermal analysis, Thermography of electric motors, Convolutional neural networks, Intelligent maintenance system, Industry 4.0.

1. INTRODUCTION

The development and use of monitoring systems capable of providing information about the operating state of the machinery and components play a critical role in a condition-based maintenance strategy, focusing on the operation's reliability and safety and reducing costs. In this context, and considering the need for a non-invasive approach, several non-destructive evaluation techniques were developed, such as eddy current, shearography, magnetic particles, acoustic emission, thermography, dye penetrant inspection, and ultrasonic and vibration-based methods.

Infrared thermography has been widely used in several situations due to its efficiency, cost, and possible integration into an intelligent monitoring system. Applications of the method include m~~M~~onitoring of fouling in heat exchangers [1], development of cracks in construction stones [2, 3], detection of delamination in reinforced concrete bridges[4], defects in post-tensioned tendon ducts [5] and in nuclear fuels [6] and as a tool to validate a heat transfer model of a roots blower [7].

Electric motors are used in several industrial segments. Detection of a failure in such types of machinery promptly provides a reliable and safe operation process and, beyond, avoids waste of sources [8]. Furthermore, the heat transfer phenomena in such machines can be used for failure detection by comparing the thermographic data at the non-damage and damage conditions, which enables the use of infrared thermography for fault detection purposes.

The infrared thermography was applied by [9] for failure detection in a 3-phase induction motor, whose results were promising. In [8], it was used an approach based on a convolutional neural network (CNN), clustering with k-means, and failure classification by Support Vector Machine (SVM) from thermographic data.

Thermograms obtained by infrared camera~~ss,~~ due to being an image of the observed phenomena, have been used in deep learning techniques to improve damage detection and establish an automatic system for identifying and classifying damages. The application of Convolutional Neural Networks (CNN), a deep learning technique, has been explored to determine the conditions of rotating machines [10, 11]. Also, detecting damages in photovoltaic panels [12, 13] and monitoring the Selective Laser Sintering (SLS) process [14]. For structural issues, [15] and [16] studied the health monitoring of roadways. In estimating concrete strength, [17]has contributed as [18] contributed to detecting embankment leakage.

Comment [MF1]: This sentence must be restructured to make sense

Following the monitoring of electrical motors, infrared thermography and CNN are used to detect failures in a grinding machine. The use of CNN allows the identification of modes of failure, and the approach can be used in an intelligent system, which provides quick responses so that decisions can be made promptly.

This proposal aims to demonstrate the viability of the joint use of CNN techniques with thermal analysis for follow-up and understandingof the behavior of failures in electric motors within a reduced context.

2.1 Infrared Thermography

The method is based on the thermal emissivity of a body being monitored, which indicates the capability of the material to emit energy as thermal radiation. This is a function of the material properties, wavelength, and temperature, once bodies with temperatures higher than absolute zero (0 kelvin) emit infrared radiation [6, 4], whose wavelengths are between about 700 nm and 1 mm, not detected by the human eye [3].

The energy (E) emitted by a body is related to its temperature (T) through the Stefan-Boltzmann equation (Eq. 1), where ε and σ refer to the emissivity and the Stefan-Boltzmann constant, respectively [4, 19].

$$E = \varepsilon \sigma T^4 \quad (1)$$

From the infrared radiation measured by infrared thermographic cameras, it is possible to establish the temperature profile of a body. Differences in temperature gradients in the target indicatethe presence of discontinuities in the form of pits, craters, cracks, or internal voids; once those induce a faster cooling and heating about the surrounding area, making it possible to detect them by the proper treatment of the thermograms[6].

UNDER PEER REVIEW

Infrared thermography (IRT) inspections can be performed by passive and active approaches. In the first method, the material being monitored is evaluated in qualitative terms, providing information about the presence or not of defects. However, in the latter approach, the target is excited by a source (e.g., laser, microwave), which results in its heating or cooling, thus making it possible to obtain quantitative data since the heating or cooling features of the excited source are characterized [2, 4, 20]. Nevertheless~~, due to its complexity,~~ the active approach is less applied than the passive onedue to its complexity, mainly in monitoring structures in the field.

2.1 Convolutional Neural Networks

Several Machine Learning and Deep Learning techniques have been used in conjunction with monitoring techniques in recent years [21-24]. CNN is a deep learning technique capable of extracting the features and differentiating the data between several conditions, being used for a wide range of image classifications [11]. A CNN model consists of several layers, among which the main ones are convolution and fully connected. In the beginning, it contains a set of filters that performs the extraction of the features of the input images according to a selected kernel. Then, flattening operations and dense layers integratethe features extracted from the previous layers. Thisresults in a feature vector for classification, whose dimensions are related to the number of classes to be classified [10, 11, 25].

In a traditional structure of a CNN model, the convolutional layer is followed by a batch normalization one, which reduces the shift of internal covariance, accelerating the training process of the deep network. Also, the convolution layer can be succeeded by an activation consisting of nonlinear functions (e.g.,hyperbolic tangent, sigmoid, and Rectified Liner Unit - ReLU), aiming to accelerate the convergence of the CNN. In the sequence, usually, it's defined a pooling layer where it's done the reduction of the dimensions of the obtained feature map in the function of the pooling size and the selected method (e.g., maximum, average, or summation pooling), keeping constant the feature map count, reducing the calculation cost and controlling the over-fitting. Next, it's linked to the fully connected layer and the softmax regression, which performs a probabilistic classification [10, 11].

2. METHODOLOGY

To evaluate the deep learning technique associated with thermographic analysis, an experimental procedure was proposed to overheat an electric motor in a controlled manner without causing permanent damage to the equipment. Thus, the electric motor used was a bench grinder, as shown in Fig. 1. To modify the temperature profile of the motor, a resistive load was applied to rotation on the right axis of the equipment.

UNDER PEER REVIEW

Fig. 1.Bench grinder used in the overheating study.

An HTI thermographic camera, model HT02, with an image resolution of 60x60 (3600 pixels), was used to obtain thermographic images. The following parameters were used for image acquisition: Ambient temperature: 27°C (measured with another thermometer); Emissivity: 0.95 (painted metallic surface, according to the device manual); Relative air humidity: 21%.

After acquiring several photos in the two operating conditions of the grinder: without load and with load, they were used to train a condition classification model based on a convolutional neural network. This neural network was responsible for evaluating the standard temperature profiles for each operational condition of the grinder.

However, a primary pre-processing step was required before building a classification model. Figure 2 presents the images obtained during the experimental procedure for collecting thermographic photographs.

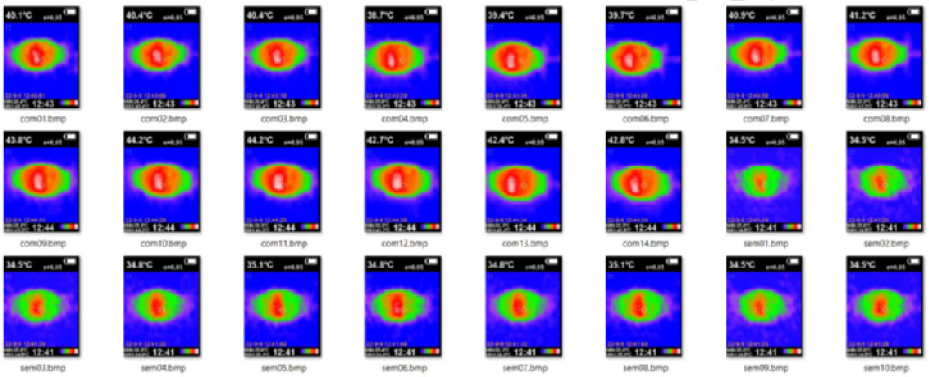

Fig.2.Thermographic images obtained from the bench grinder with and without load.

As can be seen in general, the images obtained by thermography allow the identification of two different temperature profiles of the monitored component subjectively and humanly. Since the temperature profiles are already sufficient to interpret the equipment's stress condition clearly in this work, the color tones were not readjusted in scale.

This procedure should be performed if both behaviors had very similar temperature profiles during the data sampling process but with different scales and temperature ranges. This type of thermographic camera automatically adjusts the color tones to the range of temperatures occurring on the screen. If the motor presented a similar image for both conditions, varying the temperature range, for example, from 28 to 35 °C for the no-load case but 40 to 50 °C for the load condition, it would be necessary to normalize the data to that both color profiles look distinct. This additional task would not add relevant complexity because there are already several normalization and standardization functions in the sci-kit learn library, also used in this contribution for the data separation step in training and testing.

Since the raw data, in this case, were based on manual collections from a portable device, a data pre-processing step was necessary. The images were initially converted from the standard three-layer RGB (red, green, blue) to a single layer of 256 shades of gray. Then, the image removes the header and footer with information not used for the model's decision-

making because it is not part of the thermal image of the electrical motor. Figure 3 illustrates a thermographic image obtained and the superimposition of the motor to visualize its positioning.

Fig.3.Image taken by the thermographic camera.

In Fig.3, it is possible to see the option of the camera to superimpose the thermal images on the actual image of the object to facilitate the positioning of the tripod to take pictures. However, due to the low mass of the bench, it suffered small displacements from the base caused by engine rotation. Nevertheless, this noise did not impact the classification step of the temperature profiles.

Still, in Fig.3, there is no significant color variation when it is turned off or at the beginning of the motor rotation. To reinforce this point, Fig.4 is presented, a photo taken shortly before Fig.3, removing the overlap of the actual image.

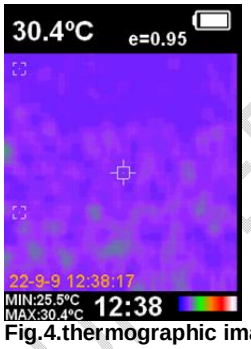

Fig.4.thermographic image at the start of the electric motor.

As expected, Fig.4 presents a homogeneous color pattern since the motor is turned off and its temperature is in thermal equilibrium with the environment.After a few seconds of rotation, the motor overheats forming the temperature profile without applying load.

UNDER PEER REVIEW

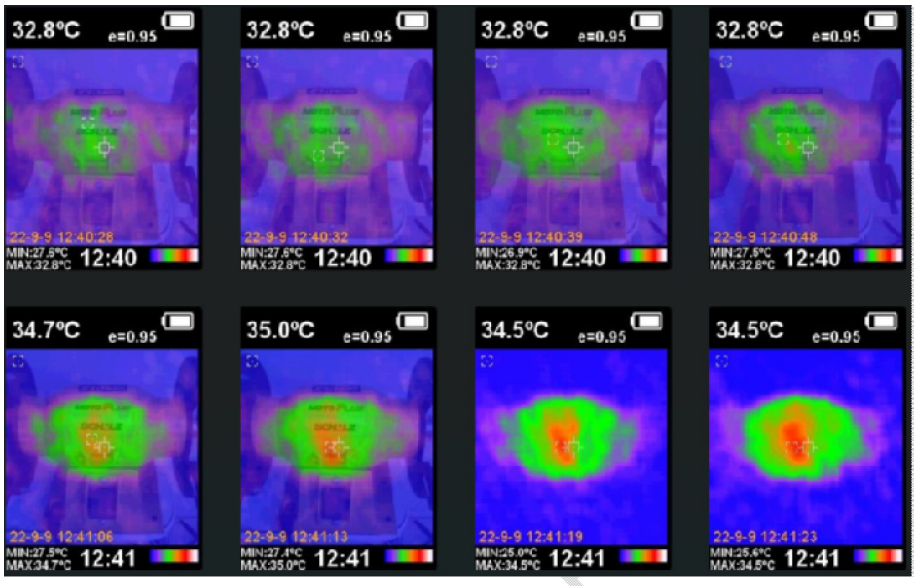

Fig.5.thermographic photos showing the temperature evolution of the engine at rest until the operation without load.

As can be seen from the color scale at the bottom of the thermal pictures and by overlay, the green temperature profile still represents a lower temperature pattern, with the center of the motor experiencing the most heating. If the motor had some leakage of charges, ~~or~~ wear, or increasing friction in rotation close to the bearings, these details would also represent hot spots in the images. However, the limited and non-destructive procedure adopted in this study was limited to applying a frictional load on the axis on the right side of the image, promoting a greater demand on the motor and thus causing overheating in Fig.2.

A binary classification model based on convolutional neural networks was constructed with images obtained from loaded and unloaded profiles on the grinder. Images obtained after pre-processing were used as input parameters for the model. This pre-processing first consisted of transforming the RGB color pattern (three layers of colors) into one of 256 levels of gray. Then remove the header and footer from the image shown in Fig.3. Figure 6 illustrates this sequence of pre-processing steps.

UNDER PEER

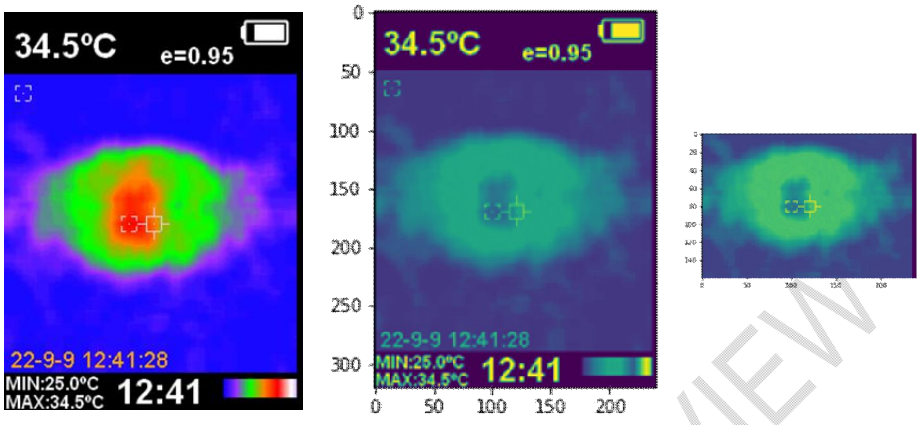

a) Original picture b) Color change c) Window selection

Fig.6.Pre-processing of images with header and footer removal.

After pre-processing the sample images, the model based on a convolutional neural network was implemented using the Keras library recently included within TensorFlow for Python language and is discussed in the next section.

3. RESULTS AND DISCUSSION

The CNN-based model uses 256 grayscale images in a 160x240 pixel matrix as inputs. The model's topologycomprised three 2D convolutional layers, with 32, 64, and 64 neurons, respectively. In all of them, the activation function was ReLU using weight initialization by the Uniform He function. After performing the resizing by a Flatten layer, the model connects to a fully connected layer with 100 neurons and is then directed to another output layer with only two neurons. In this last layer, a Softmax activation function was used due to the classification decision-making process, indicating the percentage of chances of being included in the group of images without or with the load.

The model still used the k-fold evaluation process in which ten executions of the entire process were carried out to survey the metrics and adjustments of the model to ensure its convergence and optimal results. The model's result metric was accuracy (the ability to predict correctly), and the loss function used for the training process was categorical cross-entropy, as it is a classification process.

Of the total set of 240 samples, 100 images without load and 140 with load, 33% of the data were used for testing and the rest for model training.
Thirty epochs of training were performed in each execution, using batches of size 3 for readjusting the weights. The optimization function used in the training process was ADAM, an algorithm with an adaptive learning rate. This function is generally used because it has a lower computational time for convergence in gradient-based problems, in addition to a smaller number of parameters for calibration, and is based on two other established techniques: AdaGrad and RMSProp.Figure 7 presents the graph of the ~~l~~Loss ~~f~~Function and ~~a~~Accuracy along the training steps.

UNDER PEER REVIEW

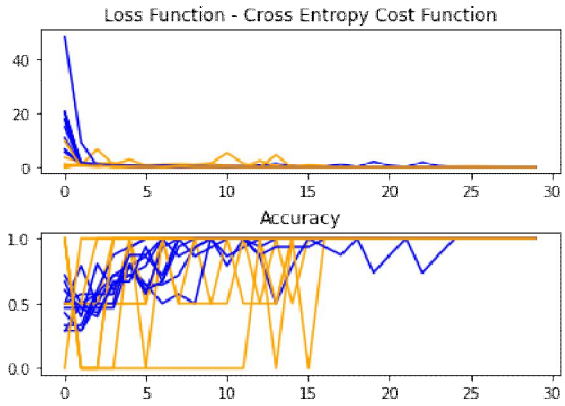

Fig.7.Results obtained with the CNN model.

The curves in blue are training data, and in orange are test data. The Loss Function only makes sense in the training stage because it adjusts the weights. However, during this modeling step, it is common to present test and training data for verification. In both cases, in the lLoss fFunction graph, it is possible to see that the values achieved converge to low values over the epochs, tending to zero when they reach epoch 10.

In the aAccuracy graph, it is possible to notice a hit of 1.0 (100%) for both training and test data after 20 epochs. This shows that after building the model, it has obtained a capacity of 100% of the correctness of an image, correctly classifying it between a motor with load or without.

For this type of evaluation of a binary classification model, it is common to use a confusion matrix illustrating the results. However, due to the results achieved with the model, with a clear distinction between the monitored conditions, there were no false positives or negatives (type I and II errors). Therefore, representing this result in a confusion matrix is unnecessary.

4. CONCLUSION

Maintenance has always been one of the highest costs in the industrial environment. However, in recent years, a greater demand for planning and availability of equipment associated with the new concepts of industry 4.0 has increased the capacity and need for maintenance. As a result, theidea of pPrescriptive mMaintenance emerges with Industry 4.0. It increases the level of Predictive Maintenance requests, monitoring the condition of items and reconciling with concepts of IoT, Big Data, Cloud Computing, and Artificial Intelligence.

As already mentioned, the study in question qualitatively showed at the beginning that the engine temperature patterns under load and no load conditions were different, facilitating the pre-processing step. In addition, the number of evaluated conditions was limited to non-destructive equipment conditions, as they were only assessed with and without load application to cause overheating. In this way, the reduced set of samples was also facilitated. Of course, for conditions in which different sources of damage are sought to be

UNDER PEER REVIEW

evaluated, such as leakage of electrical charges dissipating and promoting the joule effect or wear in bearings causing friction, new destructive cases in the equipment are necessary. Still, the temperature profile is expected todiffer from the two already presented here. Thus, the assumptions and procedures used in this study will also apply under these conditions.
As for the model obtained, some characteristics that may suggest overfitting can be noticed. This is due to the reduced number of samples used in the study, which was also justified by the low qualitative variability between samples. However, as the accuracy graph shows, after more iterations, the test sets also tend to obtain the same results as the training sample group.

UNDER PEER REVIEW

REFERENCES

1. Berce J, Zupančič M, Može M, Golobič I. Infrared thermography observations of crystallization fouling in a plate heat exchanger. ApplTherm Eng. 2023;224:120116. DOI 10.1016/j.applthermaleng.2023.120116.
2. Vazquez P, Thomachot-Schneider C. Infrared thermography as a tool to detect increasing cracking in granitic stones exposed to high temperatures. J Cult Herit. 2023;59:163-70. DOI 10.1016/j.culher.2022.11.015.
3. Hatir ME, İnce İ, Bozkurt F. Investigation of the effect of microclimatic environment in historical buildings via infrared thermography. J Build Eng. 2022;57:104916. DOI 10.1016/j.jobe.2022.104916.
4. Ichi E, Dorafshan S. Effectiveness of infrared thermography for delamination detection in reinforced concrete bridge decks. Autom Constr. 2022;142:104523. DOI 10.1016/j.autcon.2022.104523.
5. Li S, Han S, Wang J, Han X, Zheng P, Cui C et al. Infrared thermography detection of grouting defects in external post-tensioned tendon ducts under construction hydration heat excitation. NDT E Int. 2023;134:102785. DOI 10.1016/j.ndteint.2022.102785.
6. Pearlman M, Lupercio A, Rektor A, Lamb J, Fleming A, Jaques B et al. Infrared thermography method to detect cracking of nuclear fuels in real-time. NuclEng Des. 2023;405:112196. DOI 10.1016/j.nucengdes.2023.112196.
7. Matuzović M, Rane S, Patel B, Kovačević A, Tuković Ž. Analysis of conjugate heat transfer in a roots blower and validation with infrared thermography. Int J Thermofluids. 2022;16:100234. DOI 10.1016/j.ijft.2022.100234.
8. Khanjani M, Ezoji M. Electrical fault detection in three-phase induction motor using deep network-based features of thermograms. Measurement. 2021;173:108622. DOI 10.1016/j.measurement.2020.108622.
9. Jeffali F, Ouariach A, Kihel BE, Nougaoui A. Diagnosis of three-phase induction motor and the impact on the kinematic chain using non-destructive technique of infrared thermography. Infrared Phys Technol. 2019;102:102970. DOI 10.1016/j.infrared.2019.07.001.
10. Choudhary A, Mian T, Fatima S. Convolutional neural network based bearing fault diagnosis of rotating machine using thermal images. Measurement. 2021;176:109196. DOI 10.1016/j.measurement.2021.109196.
11. Li Y, Du X, Wan F, Wang X, Yu H. Rotating machinery fault diagnosis based on convolutional neural network and infrared thermal imaging. Chinese J Aeronaut. 2020;33(2):427-38. DOI 10.1016/j.cja.2019.08.014.
12. Et-taleby A, Chaibi Y, Allouhi A, Boussetta M, Benslimane M. A combined convolutional neural network model and support vector machine technique for fault detection and classification based on electroluminescence images of photovoltaic modules. Sustain Energy, Grids Netw. 2022;32:100946. DOI 10.1016/j.segan.2022.100946.
13. Mellit A. An embedded solution for fault detection and diagnosis of photovoltaic modules using thermographic images and deep convolutional neural networks. EngApplArtifIntell. 2022;116:105459. DOI 10.1016/j.engappai.2022.105459.
14. Klamert V, Schmid-Kietreiber M, Bublin M. A deep learning approach for real time process monitoring and curling defect detection in Selective Laser Sintering by infrared thermography and convolutional neural networks. Procedia CIRP. 2022;111:317-20. DOI 10.1016/j.procir.2022.08.030.
15. Kulkarni NN, Raisi K, Valente NA, Benoit J, Yu T, Sabato A. Deep learning augmented infrared thermography for unmanned aerial vehicles structural health monitoring of roadways. Autom Constr. 2023;148:104784. DOI 10.1016/j.autcon.2023.104784.

UNDER PEER REVIEW

16. Liu F, Liu J, Wang L. Asphalt pavement fatigue crack severity classification by infrared thermography and deep learning. Autom Constr. 2022;143:104575. DOI 10.1016/j.autcon.2022.104575.
17. Woldeamanuel MM, Kim T, Cho S, Kim H-K. Estimation of concrete strength using thermography integrated with deep-learning-based image segmentation: Case studies and economic analysis. Expert Syst Appl. 2023;213:119249. DOI 10.1016/j.eswa.2022.119249.
18. Zhou R, Wen Z, Su H. Automatic recognition of earth rock embankment leakage based on UAV passive infrared thermography and deep learning. ISPRS J Photogramm Remote Sens. 2022;191:85-104. DOI 10.1016/j.isprsjprs.2022.07.009.
19. Carvalho JP, Lamim PCM, Araujo ACS, Oliveira JF, Moreira JS. Parâmetros Relevantes Na Análise Termográfica De Um Motor de Indução Trifásico. In 14° SimpósioBrasileiro de AutomaçãoInteligente – SBAI. 2019;649-53. DOI 10.17648/sbai-2019-111206.
20. Avdelidis NP, Moropoulou A. Applications of infrared thermography for the investigation of historic structures. J Cult Herit. 2004;5(1):119-27. DOI 10.1016/j.culher.2003.07.002.
21. Rezende, SWF, Moura Jr, JRV, Neto, RMF, Gallo, CA, Steffen Jr, V. Convolutional neural network and impedance-based SHM applied to damage detection. Engineering Research Express, v. 2, p. 035031, 2020.DOI 10.1088/2631-8695/abb568.
22. Rezende, STF, Barella, BP ; Moura Jr, JRV. Damage Identification of Vehicle Brake Disks by the use of Impedance-Based SHM and Unsupervised Machine Learning Method. International Journal Of Advanced Engineering Research And Science, v. 7, p. 324-330, 2020. DOI 10.22161/ijaers.76.40.
23. Freitas, FA, Jafelice, RM, Silva, JW, Rabelo, DS, Nomelini, QSS, Moura Jr, JRV, Gallo, CA, Cunha, MJ, Ramos, JE. A new data normalization approach applied to the electromechanical impedance method using adaptive neuro-fuzzy inference system. Journal of the Brazilian Society of Mechanical Sciences and Engineering, v. 43, p. 1-20, 2021. DOI 10.1007/s40430-021-03186-z.
24. Gonçalves, DR, Moura Jr., JRV, Pereira, PEC,Mendes, MVA,Diniz-Pinto, HS.Indicator kriging for damage position prediction by the use of electromechanical impedance-based structural health monitoring. ComptesRendus. Mécanique, v. 349, p. 225-240, 2021.DOI: 10.5802/crmeca.81.
25. Ornek AH, Ceylan M, Ervural S. Health status detection of neonates using infrared thermography and deep convolutional neural networks. Infrared Phys Technol. 2019;103:103044. DOI 10.1016/j.infrared.2019.103044.

UNDER PEER REVIEW